J Mol Model (2009) 15:481–487
DOI 10.1007/s00894-008-0406-9

ORIGINAL PAPER

Understanding structural/functional properties of amidase from *Rhodococcus erythropolis* by computational approaches

Wei-Wei Han · Ying Wang · Yi-Han Zhou · Yuan Yao · Ze-Sheng Li · Yan Feng

Received: 31 May 2008 / Accepted: 24 August 2008 / Published online: 16 December 2008

Abstract The 3D structure of the amidase from *Rhodococcus erythropolis* (EC 3.5.1.4) built by homology-based modeling is presented. Propionamide and acetamide are docked to the amidase. The reaction models were used to characterize the explicit enzymatic reaction. The calculated free energy barrier at B3LYP/6-31G* level of Model A (Ser194+propionamide) is 19.72 kcal mol^{-1} in gas (6.47 kcal mol^{-1} in solution), and of Model B (Ser194+Gly193+propionamide) is 18.71 kcal mol^{-1} in gas (4.57 kcal mol^{-1} in solution). The docking results reveal that propionamide binds more strongly than acetamide due to the ethyl moiety of propionamide, which makes the carboxyl oxygen center of the substrate slightly more negative, making formation of the positively charged tetrahedral intermediate slightly easier. The quantum mechanics results demonstrate that Ser194 is essential for the acyl-intermediate, and Gly193 plays a secondary role in stabilizing acyl-intermediate formation as the NH groups of Ser194 and Gly193 form hydrogen bonds with the carbonyl oxygen of propionamide. The new structural and mechanistic insights gained from this computational study should be useful in elucidating the detailed structures and mechanisms of amidase and other homologous members of the amidase signature family.

W.-W. Han · Y. Wang · Y.-H. Zhou · Y. Yao · Z.-S. Li (✉)
Institute of Theoretical Chemistry, State Key Laboratory of Theoretical and Computational Chemistry, Jilin University, Changchun 130023, People's Republic of China
e-mail: zeshengli@mail.jlu.edu.cn

W.-W. Han · Y. Feng (✉)
The Key Laboratory for Molecular Enzymology and Engineering of the Ministry of Education, Jilin University, Changchun 130023, People's Republic of China
e-mail: yfeng@mail.jlu.edu.cn

Keywords Amidase · Docking · Homology modeling · Quantum mechanical calculation

Introduction

Nitrile hydratase, which catalyzes the hydration of various nitrile compounds to the corresponding amides and organic acids, is used for industrial enzymatic production of acrylamide [1]. In addition, bioconversions can be stereospecific and lead to the production of a single enantiomer, which might be a crucial aspect in the manufacturing of active new drugs [2]. Thus, the potential of these enzymes was recognized several years ago [1, 2]. Some bacteria, among them *Rhodococcus erythropolis*, can adopt short-chain aliphatic amides as sources of nitrogen for growth by virtue of their ability to hydrolyze these amides to ammonia and the corresponding organic acid [3, 4]. The amidase from *R. erythropolis* (EC 3.5.1.4) has been characterized and its primary structure with 521 amino acids determined [1]. Experimental results have shown that this enzyme can hydrolyze propionamide efficiently, and also acetamide, acrylamide and indoleacetamide at a lower efficiency; Ser194 of amidase is thought to function as the catalytic nucleophile [1, 2, 5, 6]. Furthermore, *R. erythropolis* amidase is reported to belong to a group of enzymes that contain a conserved stretch of about 130 amino acids and are designated as amidase signature (AS) family enzymes [1, 2, 5, 6]. The AS family is widespread in nature, ranging from bacteria to humans, and exhibits a variety of biological functions [2, 7, 8]. Although this family of enzymes maintains the same core structure and the same unique catalytic triad (Ser-cisSer-Lys), it has diverged to acquire a wide spectrum of individual substrate specificity. The reason for this may lie in the fact that the catalytic

power of AS family enzymes relies not only on the nature of the residues that aid catalysis but also on their position relative to the substrate. Thus, a knowledge of the three-dimensional (3D) structure of these proteins is important in understanding substrate specificity and the catalytic mechanics of the AS family. It is possible to deduce the 3D structure of amidase from *R. erythropolis* from a known function with sequence homology.

In this paper, a 3D model of amidase was constructed by a homology modeling procedure based on the crystal structure of glutamine amidotransferase CAB (GatCAB) (PDB code 2DF4) [9]. Our data support the catalytic role of Ser194, and, in all systems studied, the backbone NH of Ser194 and Gly193 create an oxyanion hole by hydrogen bonding to the oxygen of propionamide, thus stabilizing the tetrahedral intermediate. The new structural and mechanistic insights gained from this computational study should be valuable in elucidating the detailed structures and mechanisms of amidase and other homologous members of the AS family.

Theory and methods

Target and template protein

The amino acid sequence of the target protein, amidase from *Rhodococcus erythropolis* (EC 3.5.1.4), was obtained from UniProtKB-Swiss-Prot (Accession No. P22984) and 521 residues were involved [1]. The template protein was glutamine amidotransferase CAB (GatCAB) (PDB code 2DF4_A) [9].

Molecular modeling

The BLAST search algorithm was used for the online search (http://www.ncbi.nlm.nih.gov) [10]. PROTEUS2 online was employed to build the 3D structure [11]. Molecular modeling was carried out using the software Amber 9 [12]. The molecular dynamics (MD) simulation was carried out using the Amber simulation package and the Parm03 force field. The protein was solvated using a box of TIP3P [13] water molecules extending at least 10 Å away from the boundary of any protein atoms. Thus, the structure was solvated in a box of 35,858 TIP3P water molecules. An appropriate number of counterions were added to neutralize the system. The particle mesh Ewald (PME) method [14] was employed to calculate long-range electrostatics interactions. The system was gradually heated from 0 to 300 K in 15 ps with three intervals and then equilibrated for 25 ps at 300 K, followed by data collection, giving a total simulation time of 1,000 ps for amidase at 328 K. The nonbonded cutoff was set to 10.0 Å and the nonbonded pairs were updated every 25 steps. The SHAKE method [15] was applied to constrain all covalent bonds involving hydrogen atoms. The integration time step of MD calculations was 2 fs. The conformation with the lowest energy was chosen as the final model. This model was further checked by InsightII/Profile 3D and PROCHECK [16].

Docking ligands to amidase

The 3D structures of propionamide and acetamide were built via the InsightII/Builder program and were further optimized using HF/3-21G methods. Docking experiments were performed in the program AutoDock4.0 [17]. In the AutoDock4.0 docking process, a conformational search was performed using the Solis and Wets local search method, and the Lamarckian genetic algorithm (LGA) was applied to deal with enzyme–substrate interactions. Autodock calculated enzyme–ligand interaction energies over a grid; the grid size was set to 126×126×126 and the grid space was the default value of 0.375 Å. The scoring function used in the energy calculations consists of electrostatic, Lennard-Jones, hydrogen bond, salvation, and torsional entropy terms [17]. In the current version, the protein is treated as rigid while the ligand is allowed torsional flexibility.

Quantum mechanical calculation method

All calculations were performed with the Gaussian 03 program package. The first quantum mechanical (QM) subsystem (Model A) consisted of propionamide and Ser194, with a total of 25 atoms. The second subsystem (Model B) also included Model A and Gly193, leading to a total of 31 QM atoms. Density functional theory (DFT) was employed with the three-parameter hybrid exchanging functional of Becke and Lee, Yang, and Parr correlation functional (B3LYP) [18, 19]. The 6-31G* basis set was employed for all geometry optimizations. For the reactant, transition state, and tetrahedral intermediate, we further applied single-point higher-level (MP2) calculations with a larger 6-311G* basis set [20, 21] and ZPE correction was used at B3LYP/6-31g* level. The energy maximum on the path with one and only one imaginary frequency was the transition state, whereas the energy minimum along the path with no imaginary frequencies was characterized as the reactant or the intermediate. To consider the bulk solvent effects of the enzyme environment on the energetics of the reaction step, we used the polarizable-continuum model (PCM) [22] to calculate the Gibb's free energy of solvation for each species using its gas-phase-optimized geometry. To account for the polarization effects caused by the part of the surrounding enzyme that is not

explicitly included in the quantum model, cavity techniques can be used. This approximation assumes that the surrounding medium is a homogenous polarizable medium with some dielectric constant, usually chosen to be 2–8 for protein environments. The dielectric constant of the tetrachloride is 2.228, close to the protein environment [17]. Thus, in our calculations, a dielectric constant of 2.228 was used. We calculated the thermal correction to Gibb's free energies at a temperature of 328 K.

Results and discussion

Homology modeling of amidase

The BLAST search algorithm was used to conduct an online search (http://pir.georgetown.edu/). Three reference proteins, CAB (GatCAB) (PDB code 2DF4_A [9], glutamyl-tRNA(Gln) amidotransferase subunit A (PDB code 2GI3_A), and amidase (PDB code 2DCO_A) [22], were used to model the structure of the amidase. The homology scores compared to the target protein are 33%, 33%, and 31%, respectively (Fig. 1). As all the aligned proteins belong to the AS family, it can be assumed that amidase is a member of this protein family. A high level of sequence homology can guarantee more accurate alignment between the target sequence and the template structure. The amidase being studied is functional as a dimer [2], but the two chains are the same so we can build only one chain for further study. Thus, the most similar reference protein CAB (GatCAB) (PDB code 2DF4_A) [9] was chosen as the template for modeling the amidase. In this research, residues 1–8 and residues 512–521 of amidase are removed from the model because no homologous region occurs in GatCAB. These residues are not located near the active site. Thus, the model comprises residues 9–511.

The initial model was refined using energy minimization and MD simulation. Values for the root-mean square deviation (RMSD) from the initial structure are stable after approximately 1 ns, as shown by the fluctuations stabilizing around average values (Fig. 2) indicating that the trajectories have equilibrated. The conformation with the lowest energy was chosen, and the 3D structure superimposed on that of GatCAB (PDB code 2DF4_A) [9]. The RMSD value was 0.47 Å. The final structure was further evaluated for overall quality by Profile-3D. Profile-3D analysis of the model of this enzyme gave a value of 177, compared with an overall self-compatibility score of 238, and a lowest possible score of 106. This is a high figure, indicating high probability that the model is correct. Only residues Pro403–Tyr409 are built poorly and should be considered as unreliable. Fortunately, these seven unreliable residues are locate far from the active site of amidase, and would thus

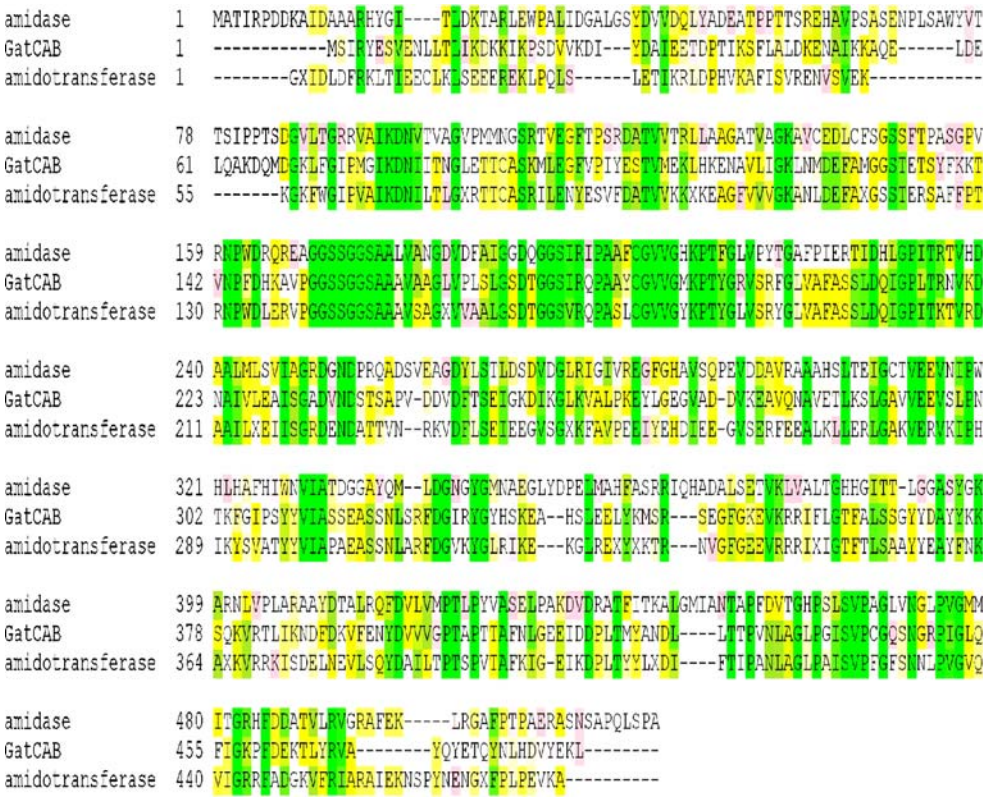

Fig. 1 Amino acid sequence alignment of three amidase signature (AS) family enzymes: *amidase* amidase from *Rhodococcus erythropolis* (EC 3.5.1.4; PDB code 2DCO_A); *GatCAB* glutamine amidotransferase CAB (PDB code 2DF4_A) [9]; *amidotransferase* glutamyl-tRNA(Gln) amidotransferase subunit A (PDB code 2GI3_A)

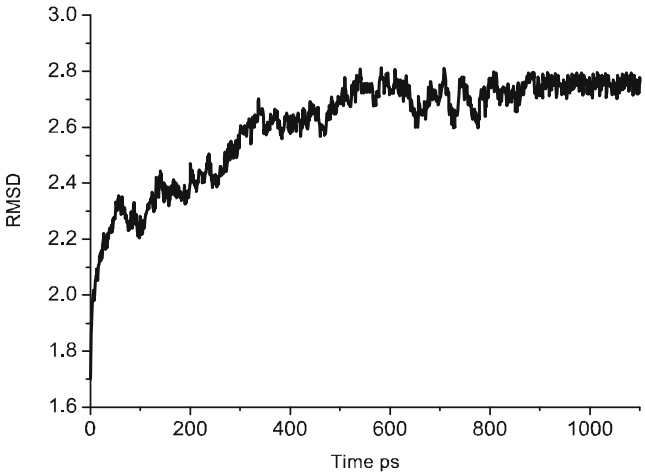

Fig. 2 Root-mean square deviations (RMSD) obtained from the 1 ns molecular dynamics (MD) trajectory for amidase

not have much influence on the present study. The final structure was evaluated using PROCHECK [16]. Among the 493 residues, the statistical score of a Ramachandran plot shows that 86.7% lie in the most favored regions, 10.2% in the additional allowed regions, 1.4% in generously allowed regions, and 0.7% in the disallowed regions. Three residues (Arg119, Lys434 and Ser146) are found in the disallowed regions of the Ramachandran plot. When their phi and psi angles are fixed manually in the conformer obtained from MD calculations, they are observed in generously allowed regions. Through this assessment and analysis process, we can conclude that the final 3D structure is reliable.

Docking study

We next used the 3D structural model of amidase to investigate docking of propionamide and acetamide to this amidase. The results may be useful in explaining why amidase hydrolyzes propionamide efficiently, and hydrolyzes acetamide at a lower efficiency [1].

We used AutoDock 4.0 to investigate substrate specificity. Most of the binding configurations predicted by AutoDock were found to be very similar, so the one with the lowest free energy was adopted. The new score function was sufficient to rank the ligands on the level of binding affinity, i.e., binding free energy ($\Delta G_{binding}$). The $\Delta G_{binding}$ between amidase and propionamide is −5.50 kcal mol^{-1} calculated by AutoDock 4.0, and $\Delta G_{binding}$ between amidase and acetamide is −3.63 kcal mol^{-1}, i.e., $\Delta G_{binding}$ between amidase and propionamide is lower than that of acetamides. Thus, propionamide binds tightly to amidase, facilitating the hydrolysis reaction. Therefore, this difference can explain the specific substrate preference of the enzyme for propionamide over acetamide.

In order to explain how amidase hydrolyzes propionamide efficiently, and hydrolyzes acetamide at a lower efficiency, we optimized the 3D structure of propionamide and acetamide using B3LYP/6-31G* methods. As listed in Table 1, the Mulliken charge on the carboxyl oxygen of propionamide is −0.51, while the Mulliken charge on the carboxyl oxygen of acetamide is −0.49. The Mulliken charge on the carboxyl carbon of propionamide is 0.59 compared with 0.58 in acetamide. It is well known that ethyl moieties are better electron donors than methyl moieties, thus the ethyl moiety of propionamide makes the carboxyl oxygen center of the substrate slightly more negative, which makes formation of the positively charged tetrahedral intermediate slightly easier. When the active site pocket is large enough to accomodate both small substrates (propionamide and acetamide), the nucleophilic Ser194 may attack the carboxyl carbon of propionamide more easily. These results are in agreement with kinetic experiments performed with amidase purified from *Escherichia coli* cells, which has a substrate specificity similar to that of amidase from *R. erythropolis* [3].

Quantum mechanical calculation

Analysis of the model structure of *R. erythropolis* amidase reveals that the active site of the enzyme is composed mainly of Ser194, Ser170, and Lys95 (Fig. 3). The enzymatic hydrolysis of amides to ammonia and the corresponding organic acid follows a two-step process. Our interest in this paper is in the first step: the formation of an enzyme–ester intermediate (Fig. 4).

In the present study, two quantum chemical models, ranging from 25 atoms to 31 atoms, were used. The following groups are included: (1) Model A is made up of propionamide and Ser194. (2) Model B is made up of propionamide, Ser194, and Gly193. The coordinates were taken from the lowest energy docking result, and hydrogen atoms were added manually.

Now let us turn our attention to the results calculated from Model A and Model B. The optimized transition state (TS) structure of Model A (TS_A) is shown in Fig. 5a,b. From Fig. 5a (in gas) and Fig. 5b (in solution), it can be seen that the NH group of Ser194 forms hydrogen bonds with the carboxyl oxygen group of propionamide in the TS. This hydrogen bonding interaction may provide sufficient stabilization of the oxyanion to generate the activity. The

Table 1 Mulliken atomic charges with propionamide and acetamide

Ligand	C_1	O_1	N
Propionamide	0.59	−0.51	−0.76
Acetamide	0.58	−0.49	−0.74

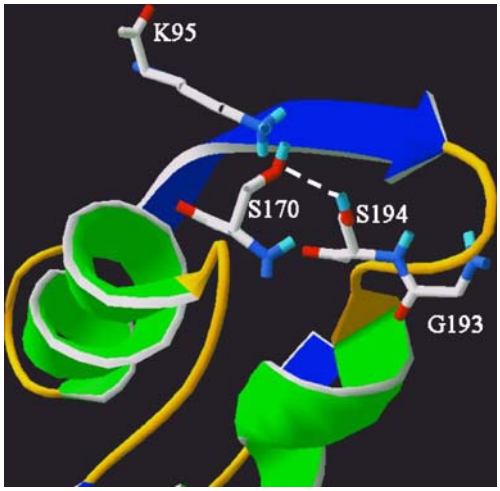

Fig. 3 The active site residues of amidase. Ser194, Ser170 and Lys95 form the catalytic triad of amidase. Gly193 is near the active site pocket

distance of C1=O1 of propionamide in TS_A is 1.28 Å in gas (1.27 Å in solution), and the regular C1=O1 bond length of propionamide in the reactants is 1.22 Å in gas (1.23 Å in solution). The distance of C1=O1 of propionamide in TS_A is elongated by about 4.69% in gas (3.15% in solution) in comparison with the bond length of C1=O1 in the reactant. The distance of C1–N of propionamide in TS_A is 1.43 Å in gas (1.44 Å in solution), and the regular C1–N bond length of propionamide in the reactant is 1.37 Å in gas (1.36 Å in solution). It can be seen that the distance of C1–N of propionamide in TS_A is longer than the bond length of C1–N in the reactant by about 4.20% in gas (5.56% in solution).

The free energy barrier heights, ΔG (the energy difference between the TS and the reactants), which was calculated at the B3LYP/6-31G* level of theory, are shown in Fig. 6a. It can be seen that ΔG is 19.72 kcal mol^{-1} in gas, which is 13.25 kcal mol^{-1} higher than that in solution. The reaction in solution is thus more favorable than that in gas. Mulliken population analysis confirms the following result: the O1 bears a charge of −0.57 at the TS in gas, while in solution the charge is −0.64 (seen from Table 1).

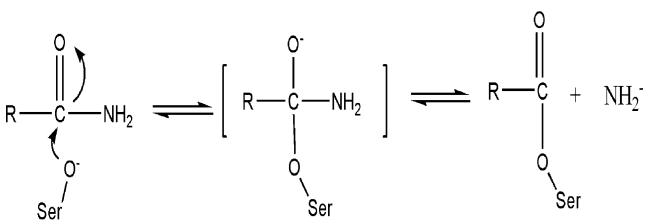

Fig. 4 Proposed mechanisms for the catalysis of propionamide and acetamide by amidase

This means that in solution the oxygen center of propionamide is slightly more negative than it is in gas, which makes formation of the positively charged tetrahedral intermediate group easier in solution. This step is calculated to be exothermic by 6.96 kcal mol^{-1}, and PCM calculation shows that the protein environment will increase the exothermicity up to 24.09 kcal mol^{-1}.

As illustrated in Fig. 5c (Model B in gas) and Fig. 5d (Model B in solution), in TS_B the tetrahedral carbonyl oxygen forms hydrogen bonds with the backbone NH-groups of Ser194 and Gly193 in the oxyanion hole, and is located close to the plane defined by C and the backbone N atoms. For Model B, the distance between O2 of the nucleophile and C1 of propionamide is 2.00 Å in gas and 2.01 Å in solution. The C1=O1 distance of propionamide in TS_B is 1.26 Å in gas (1.25 Å in solution), and the regular C1=O1 bond length of propionamide in the reactant is 1.22 Å in gas (1.23 Å in solution). The C1=O1 distance of propionamide in TS_B is longer than the regular C1=O1 bond length of propionamide by about 3.17% in gas (1.60% in solution). The C1–N distance of propionamide in TS_B is 1.42 Å in gas (1.43 Å in solution), and the regular C1–N bond length of propionamide in the reactant is 1.37 Å in gas (1.36 Å in solution). It is obvious that the C1–N distance of propionamide in TS_B is elongated by about 3.52% in gas (4.90% in solution) in comparison with the C1–N bond length in the reactant. For TS_B, the O1···Gly193–NH distance (2.18 Å in gas and 2.20 Å in solution) is longer than the O1··· Ser194–NH distance (1.84 Å in gas and 1.87 Å in solution). This result indicates that the O1···Gly193–NH bond probably breaks first, and then the weakening of this hydrogen bond represents a step in the direction of the intermediate.

For Model B, the free energy barrier heights ΔG is 18.71 kcal mol^{-1} in gas, which is 14.14 kcal mol^{-1} higher than that in solution. This step is exothermic by 0.52 kcal mol^{-1}, and PCM calculation shows that the protein environment will increase the exothermicity to 1.43 kcal mol^{-1}. The reaction in solution is thus shown to be more favorable than that in gas. The Mulliken charge on the carboxyl oxygen of propionamide is now −0.58 in gas and −0.64 in solution at the TS (seen from Table 2). This is identical with Model A.

Compared with TS_A and TS_B in gas (or in solution), the distance of C1=O of propionamide in TS_A is larger than the bond length of C1=O in reactants by about 4.69% in gas (3.15% in solution), and the C1–N distance of propionamide in TS_A is larger than the C1–N bond length in the reactants by about 4.20% in gas (5.56% in solution). But for TS_B, the C1=O distance of propionamide in TS_B is larger than the regular C1=O bond length of propionamide by about 3.17% in gas (1.60% in solution), and the distance of C1–N of propionamide in TS_B is larger than the regular

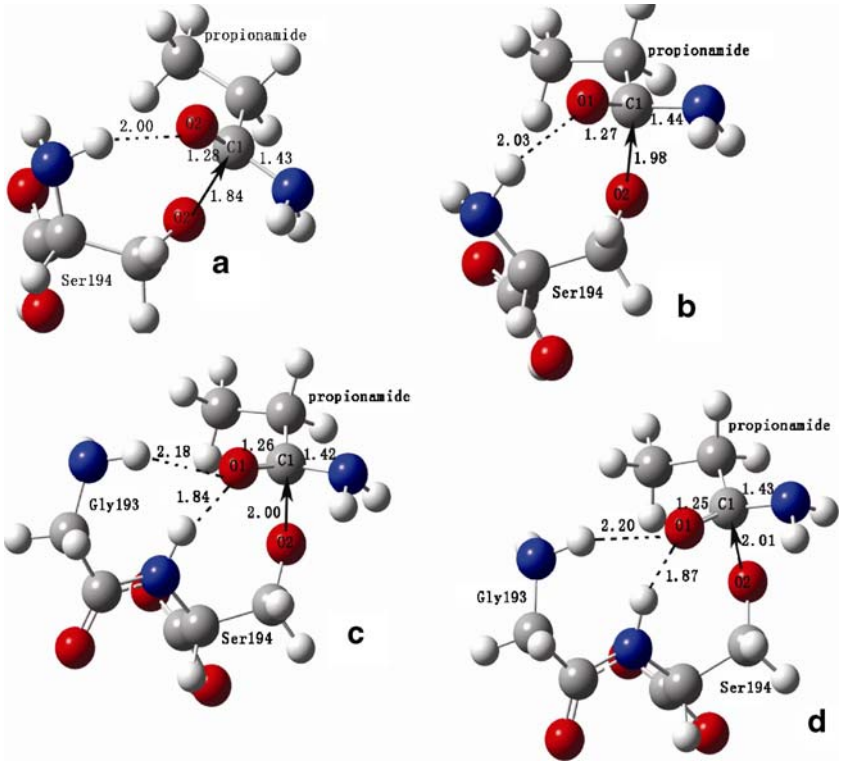

Fig. 5 Transition states (TS) located in the active site. **a** Model A in gas. **b** Model A in solution. **c** Model B in gas. **d** Model B in solution

C1–N bond length of propionamide by about 3.52% in gas (4.90% in solution). These results indicate that the barrier for Model B is closer to the reactants. Therefore, the hydrogen bond to the NH group of Gly193 makes the attack on the carbonyl carbon atom of the amide bond of propionamide slightly easier. Model B will proceed via an "earlier" TS in comparison with the same reaction with one hydrogen bond in Model A.

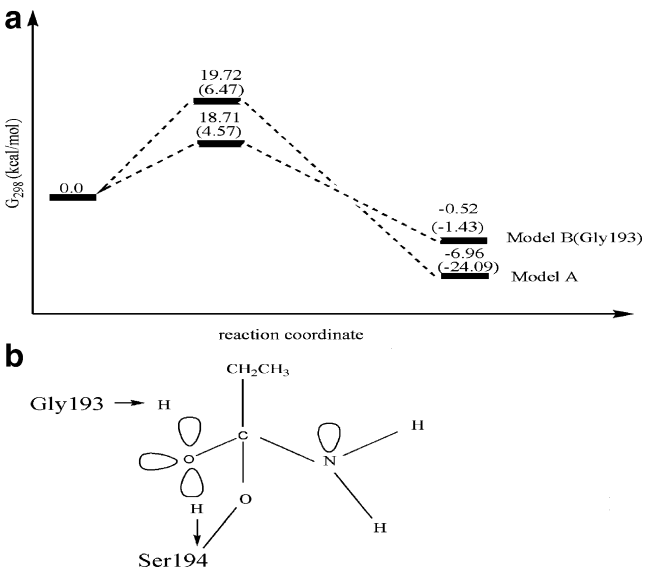

Fig. 6 **a** Free energy profiles with model A and model B in the gas phase and in the solution phase (values in parentheses). **b**. Orientation of the lone pair orbitals of the tetrahedral intermediate in the active site of amidase

From Fig. 6a, it can be seen that, without the assistance of Gly193, Model A has to overcome a free energy barrier of 19.72 kcal mol^{-1} in gas, which is 1.01 kcal mol^{-1} higher than that of Model B in gas. After the solvation energies caused by the protein electrostatic environment are considered, the barrier of Model A becomes 6.47 kcal mol^{-1}, which is 1.90 kcal mol^{-1} higher than that of Model B. Thus, the protein environment has a significant effect on the free energy barrier. As discussed above, these results show that forming an H-bond between Gly193 and propionamide will decrease this barrier.

The present results indicate the important role of Ser194 and Gly193 hydrogen bonds in the oxyanion hole. Nevertheless, it seems that Gly193 is not absolutely essential, which is not too surprising, for two reasons. First, the catalytic machinery involving Ser194, Ser170, and Lys95 has not been altered. Second, the amidase oxyanion can still form a single hydrogen bond with the

Table 2 Mulliken atomic charges in the transition states (TS) with Model A and Model B

Species	O1	C1	N	O2
Model A in gas	−0.57	0.61	−0.74	−0.62
Model A in solution	−0.64	0.61	−0.75	−0.64
Model B in gas	−0.58	0.61	−0.73	−0.64
Model B in solution	−0.64	0.61	−0.75	−0.65

NH group of Ser195 (see Model A), which can provide sufficient stabilization of the oxyanion to generate the observed low level of activity.

It was reported that hydrogen bonds to the oxyanion not only decrease the free energy barrier but also control the orientation [23, 24]. The oxyanion of the tetrahedral intermediate has three lone pairs: two are hydrogen bonded to Ser194 and Gly193, and the other is a free lone pair (Fig. 6b). It is widely known that cleavage of a C–O or C–N bond requires the assistance of an anti-periplanar lone pair orbital on each of the two remaining heteroatoms. Thus, when the tetrahedral intermediate was built up, the lone pair orbital of the leaving nitrogen and of the oxyanion must be anti-periplanar to the new C–O bond, and when the tetrahedral intermediate decomposes, the leaving group should have a lone pair orbital anti-periplanar to the C–N bond that is to be broken.

Conclusion

The 3D structure of amidase from *R. erythropolis* (EC 3.5.1.4) was obtained by homology modeling using glutamine amidotransferase CAB (GatCAB) (PDB code 2DF4_A) as a template. In this research, docking studies showed that propionamide binds more strongly than acetamide in the amidase–ligand complexes. Furthermore, a reaction model is proposed and the reaction mechanism was investigated by employing quantum mechanics calculations in both gas phase and solution. The calculated results indicate that hydrogen bond interactions may decrease the energy barrier and control the orientation of the subsequent reaction. The novel structural and mechanistic insights provided by this computational study should be useful in elucidating the detailed structures and mechanisms of amidase and other homologous members of the AS family.

Acknowledgments This work was supported by the National Science Foundation of China (20333050, 20673044), Doctor Foundation by the Ministry of Education, and Foundation for University Key Teacher by the Ministry of Education, Key subject of Science and Technology by the Ministry of Education of China, and Key subject of Science and Technology by Jilin Province.

References

1. Hashimoto Y, Nishiyama M, Ikehata O, Horinouchi S, Beppu T (1990) Biochim Biophys Acta 1088:225–233
2. Mayaux JF, Cerbelaud E, Soubrier F, Faucher D, Petre D (1990) J Bacteriol 172:6764–6773
3. Skouloubris S, Labigne AH, Reuse HD (2001) Mol Microbiol 40:596–609, doi:10.1046/j.1365-2958.2001.02400.x
4. Vliet AHMV, Stoof J, Poppelaars SW, Bereswill S, Homuth G, Kist M et al (2003) J Biol Chem 278:9052–9057, doi:10.1074/jbc.M207542200
5. Patricelli MP, Cravatt BF (2000) J Biol Chem 275:19177–19184, doi:10.1074/jbc.M001607200
6. Shin S, Yun SY, Koo HM, Kim YS, Choi KY, Oh BH (2003) J Biol Chem 278:24937–24943, doi:10.1074/jbc.M302156200
7. Shin S, Lee TH, Ha NC, Koo HMS, Kim Y, Lee H-S et al (2002) EMBO J 21:2509–2516, doi:10.1093/emboj/21.11.2509
8. Labahn J, Neumann S, Buldt G, Kula MR, Granzin J (2002) J Mol Biol 322:1053–1106, doi:10.1016/S0022-2836(02)00886-0
9. Nakamura A, Yao M, Chimnaronk S, Sakai N, Tanaka I (2006) Science 312:1954–1968, doi:10.1126/science.1127156
10. Altschul SF, Madden TL, Schäfer AA, Zhang JZ, Miller DJ (1997) Nucleic Acids Res 25:3389–3402, doi:10.1093/nar/25.17.3389
11. Montgomerie S, Cruz JA, Shrivastava S, Arndt D, Berjanskii M, Wishart DS (2008) Nucleic Acids Res 36:W202–W209
12. Case DA, Darden TA, Cheatham TE III, Simmerling CL, Wang J, Duke RE, Luo R, Merz KM, Pearlman DA, Crowley M, Walker RC, Zhang W, Wang B, Hayik S, Roitberg A, Seabra G, Wong KF, Paesani F, Wu X, Brozell S, Tsui V, Gohlke H, Yang L, Tan C, Mongan J, Hornak V, Cui G, Beroza P, Mathews DH, Schafmeister C, Ross WS, Kollman PA (2006) AMBER 9, University of California, San Francisco
13. Jorgensen MJ, Chandrasekhar J, Madura JD, Impey RW, Klein ML (1983) J Chem Phys 79:926–935, doi:10.1063/1.445869
14. Darden T, York D, Pedersen L (1993) J Chem Phys 98:10089–10092, doi:10.1063/1.464397
15. Ryckaert JP, Ciccotti G, Berendsen HJC (1977) J Comput Phys 23:327–341, doi:10.1016/0021-9991(77)90098-5
16. Luthy RA, MacArthur MW, Moss S, Thornton JM (1993) J Appl Cryst 26:283–291, doi:10.1107/S0021889892009944
17. Huey H, Morris GM, Olson AJ, Goodsell DH (2007) J Comput Chem 28:1145–1152, doi:10.1002/jcc.20634
18. Kravitz JY, Pecoraro V, Carlson HA (2005) J Chem Theory Comput 1:1265–1274, doi:10.1021/ct050132o
19. Velichkova P, Himo F (2005) J Phys Chem B 109:8216–8219, doi:10.1021/jp0443254
20. Wang JY, Dong H, Li SH, He HW (2005) J Phys Chem B 109:18644–18672
21. Li A-J, Nussinov R (1998) Proteins 32:111–127, doi:10.1002/(SICI)1097-0134(19980701)32:1<111::AID-PROT12>3.0.CO;2-H
22. Pham TC, Kriwacki RW, Parrill AL (2007) Biopolymers 86:298–310, doi:10.1002/bip.20745
23. Claiborne A, Yeh JI, Mallett TC, Luba J, Crane EJ, Charrier V et al (1999) Biochemistry 38:15407–15416, doi:10.1021/bi992025k
24. Warshel A, Naray-Szabo G, Sussman F, Hwang J-K (1989) Biochemistry 28:3629–3637, doi:10.1021/bi00435a001